UCR-02 Tractive Cooling System Report

Noah Elsayed

2024-2025 FSAE EV Season

Contents

1 Introduction

1.1 Background

Formula SAE (FSAE) is a collegiate engineering design competition wherein teams of students from universities around the world design and build formula-style race cars. The cars are raced and judged against each other, equipping students with industry-ready skills along the way. FSAE was initially limited to internal combustion engines, with an all-electric variant of the competition being introduced in 2010. These FSAE electric vehicles (EVs) offer far superior performance due to their electric motors, but come with unique challenges such as cooling and battery management.

In FSAE EVs, effective thermal management of the powertrain is crucial for ensuring performance, efficiency, and reliability. Unlike internal combustion engines, electric powertrains only produce heat when the system is under load. These losses impose thermal stress on key components such as the inverter and motor, affecting performance and longevity.

A poorly designed tractive cooling system (TCS) can result in reduced power output and, in extreme cases, component failure such as motor demagnetization. The previous cooling system on UCalgary Racing's first FSAE EV, the UCR-01, was hastily designed with little documentation, limiting both its effectiveness and ability to be built upon. Additionally, the lack of detailed design documentation hindered communication during competition design presentations, negatively impacting scoring.

1.2 Objectives

This report presents the design, development, and testing of the TCS for UCalgary Racing's second FSAE EV, the UCR-02. The system is designed to efficiently dissipate heat from the motor and inverter while adhering to strict packaging constraints and minimizing low-voltage electrical system load. The major objectives for the UCR-02 TCS include:

- Developing a cooling system capable of maintaining powertrain component temperatures within safe operating limits under dynamic load conditions
- Minimizing electrical power consumption through efficient design
- Creating and validating a thermal model to guide design decisions
- Prioritizing serviceability through accessible maintenance features and efficient bleeding procedures
- Establishing a robust methodology for performance validation that provides a framework for evaluating both this system and future systems
- Effectively incorporating sensors to inform design of future vehicles

This report aims to address the shortcomings of previous iterations by establishing a clear design foundation for future teams. The emphasis on thorough documentation throughout this project will support both future designs and competition presentations.

2 Rule Review

Before beginning any FSAE-related project, a review of all relevant rules is necessary. The 2025 FSAE rule book [1] has many rules related to the TCS, all of which are listed in this section. It is imperative that rules are reviewed and understood each year, as to account for any relevant changes.

1. Coolant Fluid Requirements

- **Rule T.5.4.2:**
  - Liquid coolant for electric motors or HV electronics must be:
    - Plain water (no additives), **or**
    - Oil

2. System Sealing & Leak Prevention

- **Rule T.5.5.1:** The cooling system must be sealed to prevent leakage.
- **Rule T.5.5.2:** The vehicle must withstand a 45° tilt without fluid leakage.

3. Catch Can Requirements

- **Rules T.5.6.1–T.5.6.4:** Vented cooling systems require catch cans that:
  - Are leak-proof (withstand boiling water)
  - Have minimum capacity of 10% of coolant volume or 0.5 L (whichever is larger)
  - Are mounted rearward of the firewall, below the driver's shoulders
  - Use rigid mounting (no zip ties)
  - Vent via a hose (min. 3 mm diameter) to the chassis bottom

4. Thermal Protection for Driver Safety

- **Rules T.1.6.1–T.1.6.3:** Cooling components must prevent driver contact with surfaces >60°C via:
  - **Conduction isolation:** 8 mm heat-resistant material or no direct contact
  - **Convection isolation:** 25 mm air gap
  - **Radiation isolation:** 0.4 mm metal shield or reflective foil

5. Open Wheel Constraints (Radiator Placement)

- **Rule V.1.1:** No part of the cooling system may intrude into the 'keep-out zone' defined by:
  - 75 mm forward/aft of the tire outer diameter
  - Lateral space between the inboard/outboard tire planes

3 Literature Review

Effective cooling is crucial for ensuring drivetrain reliability and performance in FSAE EVs. Many successful teams have documented their approaches to designing optimized cooling systems. While these resources provide valuable insights, certain oversights and limitations highlight the need for a more refined approach. Additionally, compiling the cooling systems of multiple teams offers valuable context and creates a reference point for designing the UCR-02 TCS.

Jander's documentation of RIT Racing's first FSAE EV TCS [2] offers a high-level overview of the development process, however a closer examination of the study reveals a significant oversight in the initial simulation process. The final vehicle uses a single Mishimoto 450cc dirt bike radiator [3], two Davies Craig EBP40 pumps [4], and a high-powered Sanyo Denki fan [5]. While the system was tested and found to be excessive, it is crucial to note that the radiator is housed in a vehicle sidepod, which provides better airflow than would be possible on the UCR-02. A review of the simulation script reveals that the overall heat transfer coefficient, U, was determined for a single radiator under specific conditions and then used as a general value when computing results for multiple radiators undergoing transient conditions. While basic heat transfer principles are vital in system design, the transient nature of the system invalidates this simulation methodology.

LaMarre's work on the University of Akron's FSAE EV TCS [6] provides a comprehensive breakdown of the heat transfer theory required for such a system. The design uses a custom Visteon radiator paired with a GRI INTG7 pump [7] to cool the vehicle's motor and controller. However, the report lacks empirical validation, rendering the efficacy of the specified system inconclusive and, like Jander's work, it fails to sufficiently address thermal transience. Furthermore, the pumps used are infeasible for the UCR-02 TCS, as their 300 Watt load is too high for incorporation due to the small low-voltage battery used on the UCR-02. Despite these limitations, the report offers valuable insights into determining loop parameters such as pipe diameter, which can be applied when designing an EV TCS.

Jamadar et al.'s paper [8] outlines a simulation-based approach for designing an FSAE EV TCS. The article addresses both accumulator and tractive system cooling; however, only the tractive system will be considered here. MATLAB, along with its Simulink and Simscape extensions, was used to create a comprehensive model capable of simulating the system and evaluating components. The vehicle utilizes sidepods to direct airflow toward radiators, and the system operates with a low coolant flow rate of only 6 liters per minute (lpm). Such a low flow rate allows for smaller pumps, reducing the power draw on the low-voltage system. The paper concludes by verifying the theory used with empirical results.

Finally, Chiu documented the design of MIT Motorsports' MY19 tractive cooling system [9]. While the report's methodology struggles to account for thermal transience, it correctly addresses system fluid behavior. The final system utilizes a single Mishimoto Yamaha YFM700R radiator [10] and an Everflo EF7000 diaphragm pump [11]. However, the report does not provide empirical validation, leaving the efficacy of the methodology unconfirmed. Moreover, the use of such a high-power, positive-displacement pump is unsuitable for the UCR-02 due to its high weight and 23 Amp draw.

4 System Design & Methodology

4.1 System Constraints

The first step in creating a FSAE EV TCS is determining system constraints. As TCS development began late in the UCR-02's design cycle, electrical constraints are imposed on the system that would likely be less severe in an ideally-developed car. The low-voltage electrical team designed their 12 Volt subsystem with two Davies Craig EBP23 pumps [12] and four computer fans in mind, meaning a total current draw of less than 2 Amps was expected. Due to the inherent air and liquid pressure drops present in TCS components, total system current will exceed 2 Amps by a large margin. As such, the TCS is designed with low-voltage power minimization as a priority.

The UCR-01's TCS suffered from poor bleedability, making it extremely difficult to remove all air from the system. As such, bleedability is also a priority in designing the UCR-02's TCS. As is always true in motorsport, the system is designed with weight minimization and compact packaging in mind.

The inverter used in the UCR-02 is the Bamocar D3 [13], and the motor is the Emrax 228 [14]. These components have manufacturer specified maximum inlet temperatures, minimum flow rates, and nominal pressure drops. A tabulation of component properties is available in Table 1.

Component Name	Maximum Inlet Temperature [°C]	Minimum Flow Rate [lpm]	Nominal Pressure Drop [bar]	Coolant Volume [mL]
Bamocar D3	65	6	0.56 at 10 lpm	-
Emrax 228	50	6	0.5 at 6 lpm	100

Table 1: Component Parameters

4.2 Early Design

4.2.1 Early Model

Initial development of the system was done through simple equations and basic empirical testing, resulting in a rudimentary design methodology. The initial process will not be covered here, as **using simple equations and approximations is an ineffective way of developing a TCS**. The ineffectiveness of the basic principles covered in heat transfer classes and even most heat transfer textbooks is a result of transience, wherein the system is never at thermal steady-state conditions. This invalidates most traditional methods and leads to a choice of either manually solving partial differential equations (PDEs) in 3 Dimensions over time or utilizing simulation software. Although the flawed mathematical approach will not be discussed here, the mistakes made while empirically evaluating radiator performance will be.

4.2.2 Early Testing

In the initial testing process a basic, low-quality 120mm x 240mm computer radiator was evaluated. The process consisted of heating a large quantity of water and pumping the heated water through the radiator while running fans. Initial tests yielded noisy data, but an improved, albeit fundamentally flawed process garnered some reasonable results. The latter method and its flaws are discussed here.

The apparatus used to conduct the testing is comprised of a large stockpot, a Davies Craig EBP23 pump [12], spare tubing, 2 computer fans, 2 temperature sensors, and a generic 120mm x 240mm computer radiator [15]. The tubing and pump are connected in series with the radiator, and the volume of water is heated to 75°C. With the 1500W heater left on, the system runs until the water temperature stabilizes. The flow rate is then collected using a simple timed mass test, and data analysis begins.

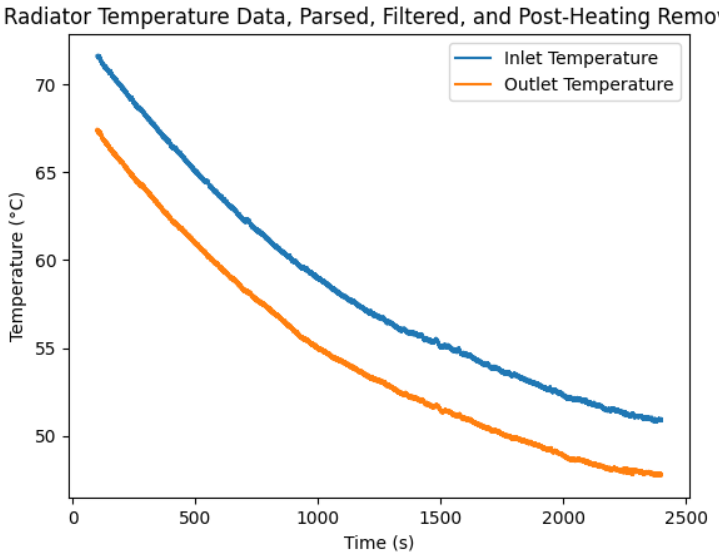

Figure 1: Processed Empirical Computer Radiator Data

The collected data is cleaned in a Jupyter notebook using Python, and the log-mean temperature difference (LMTD) is used to evaluate the radiator-fan combination. This method yields a value of hA, a term combining convective heat transfer coefficient, h, and heat transfer area, A. The hA value does not generalize to different flow, temperature, or geometry conditions and is thus somewhat irrelevant. The more appropriate effectiveness-number of transfer units (ϵ -NTU) method is thus employed.

The ϵ -NTU method allows for easier analysis of heat exchangers when only inlet temperatures are known, as is the case in an EV TCS. The ϵ -NTU method uses effectiveness, ϵ, and maximum heat transfer possible, q_{max} to calculate heat transfer at various conditions, where

$$\epsilon = \frac{q}{q_{max}}$$

and

$$q_{max} = C_{min}(T_{h,i} - T_{c,i})$$

which represents the maximum heat transfer theoretically possible in a heat exchanger. C_{min} is simply the minimum heat capacity of the two fluid streams, and $T_{h,i}$ and $T_{c,i}$ are the hot and cold stream inlet temperatures, respectively. Using Python's Coolprop library to gather all fluid properties given both local ambient and competition conditions, q and q_{max} are calculated for the range of time shown in Figure 1 to compute radiator effectiveness.

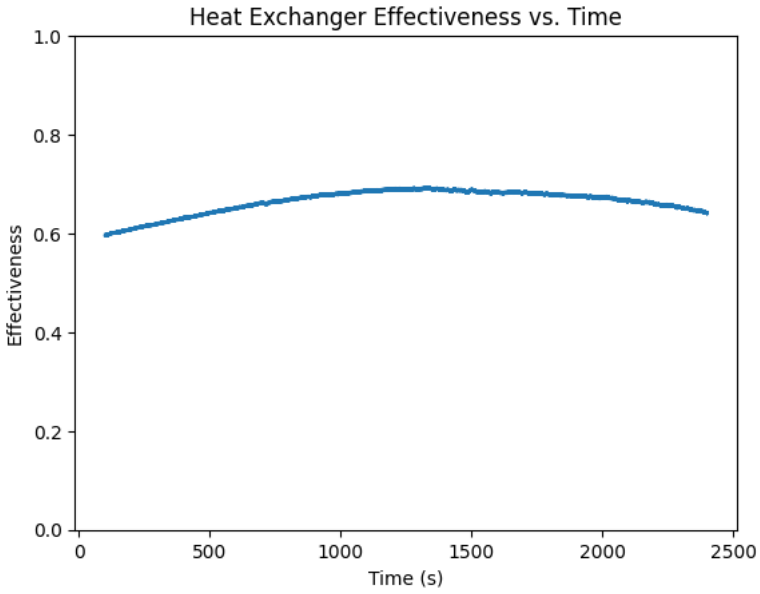

Figure 2: Computer Radiator Effectiveness-Time Plot

Radiator effectiveness should theoretically be constant with time, however the results in Figure 2 suggest the method's validity due to their low variance and relative consistency. As such, the mean effectiveness value is used to approximate that of the actual radiator. The effectiveness value is then used to find heat transfer possible at competition conditions, assumed to be 35°C ambient temperature, sea-level ambient pressure, and a maximum coolant temperature of 70°C.

$$q = \epsilon C_{min}(T_{water,in} - T_{ambient})$$

Use of the above equation yields a theoretical heat transfer of 1449.46 Watts at the competition, however there are many major flaws in the previously outlined process. The first and most major problem is the non-steady nature of the apparatus, as a considerably more accurate approach would be to have a specified volume of constant temperature fluid and pump that through the radiator into a different container. This would yield greater proximity to steady-state conditions, increasing validity. Further, the assumed operating temperature of 70°C is far higher than would be ideal at the competi-

tion, and the nature of EVs producing heat only when the system is under load means a non-constant value of vehicle heat produced, resulting in transience. Lastly, the loss of heat to the ground and surrounding air contribute to thermal losses which are not accounted for, alongside the ineffective heating of the water by the element due to its excessive temperature; when the element is too hot, a thin layer of insulating vapor forms as per the Leidenfrost effect, reducing the element's ability to heat the water.

The early method described serves to inform a more effective future testing process, and demonstrate the importance of understanding heat transfer theory before designing an EV TCS.

4.3 MATLAB Model Creation

After attempting to utilize fundamental heat transfer calculations, reviewing relevant literature, and consulting with individuals familiar with designing such a system, it is determined that a simulation and validation-oriented approach is most optimal in designing the UCR-02's TCS. The primary reason behind taking this approach is the considerable thermal transience in a TCS, which is difficult to capture using traditional methods. Furthermore, the relative simplicity of simulation software when compared with other mathematical approaches to thermal system design result in a lower likelihood of error. Extensive validation of cooling systems is often neglected in the literature and is viewed favorably by FSAE design event judges, and as such, a process of reviewing an existing simulation model, addressing any issues, and testing components before constructing the TCS is undertaken.

MATLAB, alongside its Simulink and Simscape extensions [16], is used to create the UCR-02 TCS model as it provides powerful, pre-made components with relatively straightforward configuration procedures. Mathworks also provides the software free of charge to University of Calgary students, making it accessible to team members. Further, the numerous MATLAB guides created specifically for FSAE teams [17] makes understanding the relevant modeling process simpler.

4.3.1 Previous Model

In the development cycle of the UCR-01, a MATLAB thermal simulation model was developed. This model helped inform the TCS used on the car, but was suspected to have overestimated system heat generated. Analysis of the previous model reveals considerable oversights which likely contribute to the overestimate of heat rejection required.

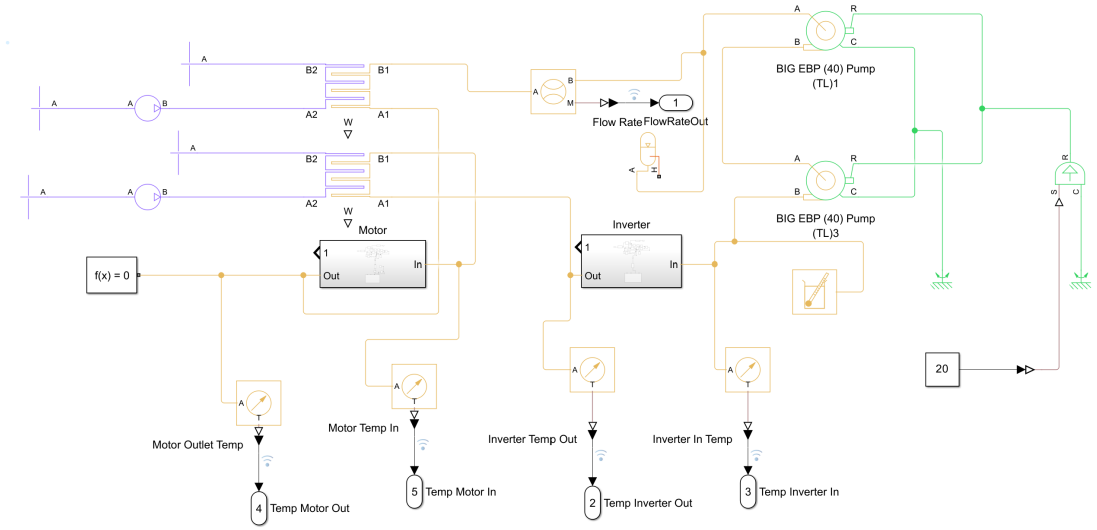

Figure 3: UCR-01 MATLAB Simulink and Simscape Model

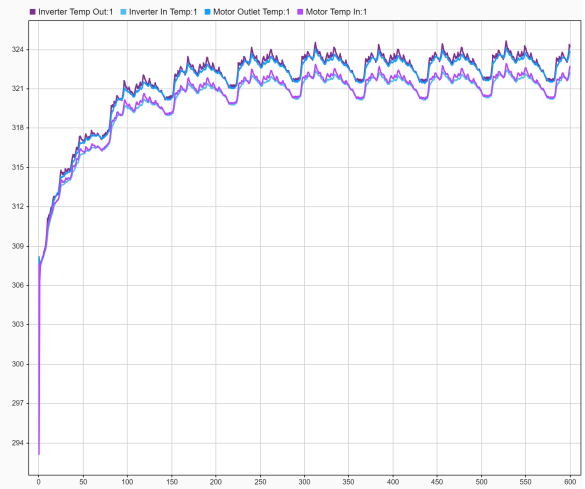

Figure 4: UCR-01 Thermal Model Results. X: Time (S), Y: Temperature (K).

The UCR-01 thermal model fails to account for component heat capacity, decreasing time required to reach a stable state. This likely contributes to the model's overestimate of heat rejection required, as the physical system's large thermal mass acts as a heat sink. The model overestimating heat produced aligns with observations gathered while testing the car, as with ambient temperatures of around 5-10°C, the system seldom overheated with no pumps or fans running. **It must be noted that this observation is not a sound basis to make design decisions and is merely a reason to review the model.** Going forward, data must be used to make decisions and **the vehicle should never be**

driven without a functioning TCS. The UCR-01 model also lacks many accurate initial conditions, causing a spike in the data. Lastly, the model fails to accurately account for the thermal capacity of the coolant, with many chamber volumes being left at default values. The UCR-01 TCS thermal model serves as a good baseline to work from, and addressing the major problems with the model allows for creation of a superior UCR-02 TCS thermal model.

4.3.2 Component Thermal Models

Creation of an accurate TCS model first entails the creation of superior motor and inverter thermal models, accounting for heat capacities and efficiencies more accurately. This requires taking pre-generated endurance event lap time simulation data and transforming it into appropriate thermal energy values. A major assumption employed is that all component inefficiency is converted to thermal energy, which is reasonable due to the highly-efficient nature of EVs and adds an inbuilt factor of safety (FOS).

The Bamocar D3 [13] was confirmed to have an average 92% efficiency by a Unitek representative. Figure 5 shows its thermal model, where vehicle power is multiplied with the 8% inefficiency and is converted into thermal energy using a heat flow rate source. The thermal mass of the component is accounted for through modeling the aluminum cooling plate, the casing, and the remaining 5 kg of unknown thermal mass. For the unknown thermal mass, an underestimated approximation of heat capacity is used. Underestimation is preferable when compared to overestimation as it increases system sensitivity to heat generation, and a system with too little sensitivity may underestimate cooling capacity required. The thermal energy conducts through the cooling plate, and heats the coolant volume of the controller which is connected to the component's coolant inlet and outlet. It can be seen in Table 1 that Unitek does not provide a specified coolant volume for the inverter, and as such manual bleeding and coolant volume measurement is done to yield a coolant volume of 200 mL.

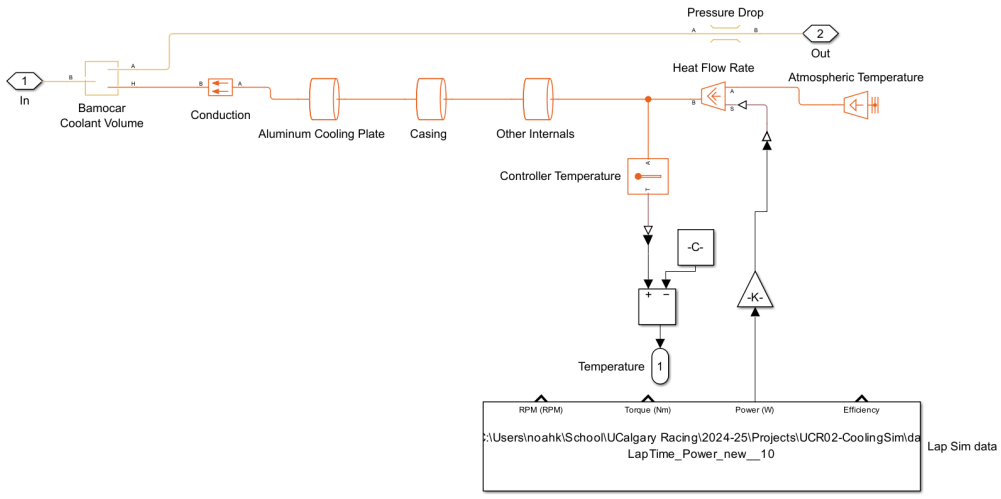

Figure 5: Bamocar D3-700 Thermal Model

The Emrax 228[14] has a manufacturer-provided efficiency map, which can be used in its thermal model. The efficiency is translated to a 3 dimensional lookup table, as shown in Figure 7. The thermal model calculates efficiency based upon motor RPM and torque, using the lookup table. The inverter's inefficiency is accounted for in the power delivered to the motor, as power is reduced by 8%. The thermal energy is sent to a 5 kg aluminum thermal mass, which is then conducted into the motor coolant volume. The use of only 5kg thermal mass despite the motor's 13kg mass is as a function of certain parts of the motor, such as the rotor, being unlikely to experience considerable heating. Again, underestimation of thermal mass is preferable to overestimation.

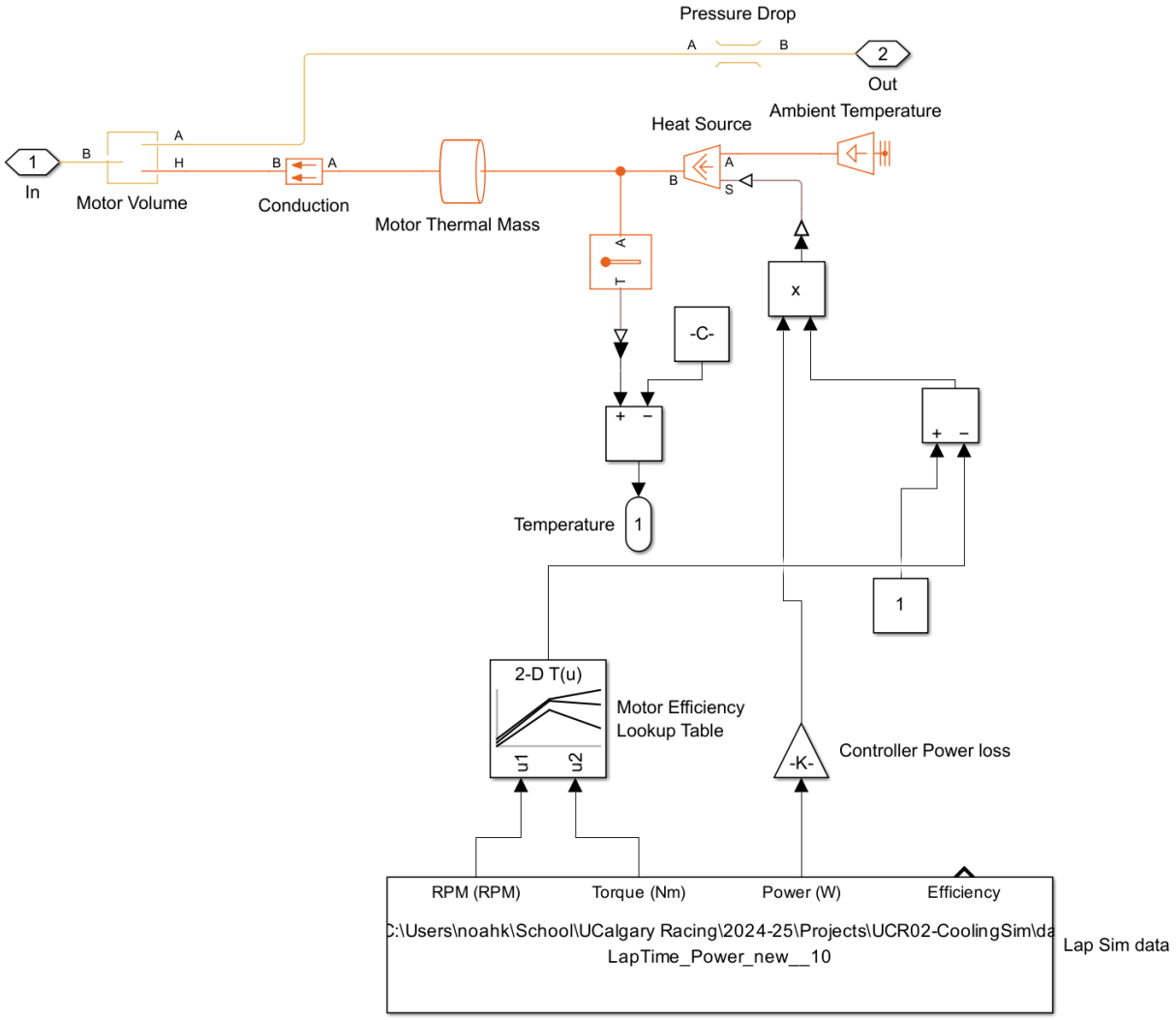

Figure 6: Emrax 228 Thermal Model

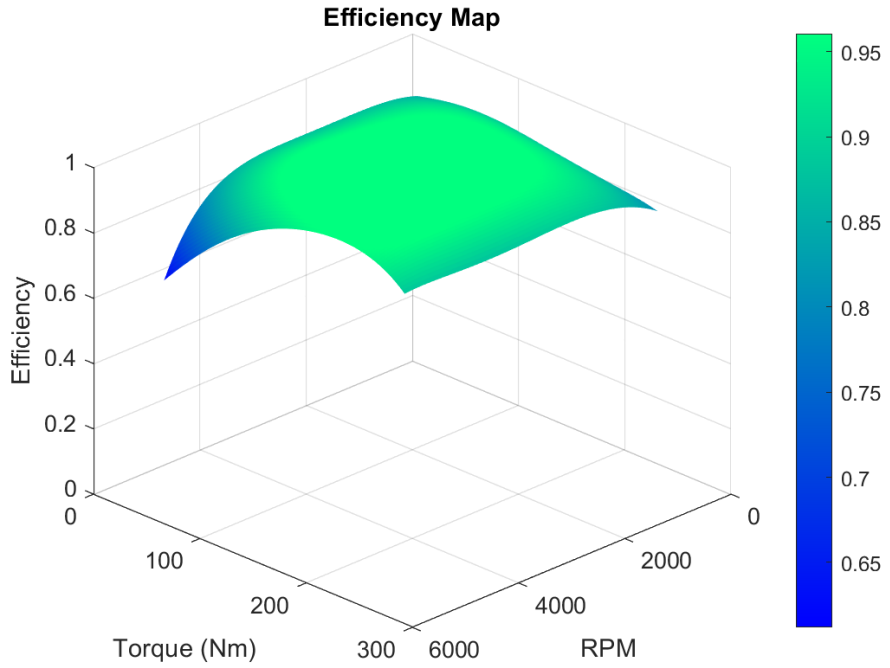

Figure 7: Emrax 228 Efficiency Plot

A major oversight of the model is the air cooling effect on both the motor and inverter, however they are extremely difficult to account for in such a model. Accurate modeling of effect of air cooling on the TCS requires complex computational fluid dynamics (CFD), which is beyond the scope of this report. As such, the effect is neglected and simply acts as an additional FOS in designing the system.

4.3.3 Radiator Modeling

Simulink makes modeling of heat exchangers such as the radiators used in a EV TCS much simpler than would otherwise be possible, as outlined by Mathworks' guide on the subject [18]. Use of the methodology outlined in the article makes transferring the physical dimensions of radiators a trivial task of core, tube, and fin measurement alongside material identification. This allows for simple creation of models such as the previously discussed computer radiator [15], a Mishimoto 450cc dirtbike radiator [19], a Mishimoto YXR700 Rhino ATV radiator [20] and the custom 200mm x 200 mm UCR-01 radiators shown in Figure 8.

Figure 8: Custom UCR-01 Radiator

4.3.4 Coolant Flow Rate Optimization

The coolant flow rate is constrained by the manufacturer specified minimum flow rates of 6 lpm for both the motor and inverter, and as a result of the requirement to minimize current draw on the vehicle low voltage system, the TCS is designed with low flow rates as a priority. This is particularly as a result of the high pressure drop in EV drivetrain components, as the small coolant cavities mean that high flow rates require considerably more pump capacity than comparable Internal Combustion Engine [ICE] powered vehicles. Although higher flow rates yield increased heat transfer, Jamadar et. al's paper [8] supports the possibility of using lower flow rates as the successful system outlined in the report successfully utilizes a 6 lpm flow rate.

4.3.5 Air Flow Rate Determination & Modeling

As a result of the late development of the UCR-02's TCS, complete aerodynamic integration of the radiators is not possible. Ideally, an optimized aerodynamic package would maximize radiator airflow through use of bodywork such as sidepods. However, the UCR-02 is limited in placing any radiators on the back of the frame, near the rear wheels. Although this placement is far from ideal, having such a constraint makes airflow to the region a known parameter. The aerodynamics subteam used CFD to determine air flow rate to the rear-placed radiator region, which was determined to be 50% of the vehicle's velocity. Inclusion of fans in the design provides superior airflow at low vehicle speeds, as the pressure difference created by fans is the dominant source of airflow. At higher vehicle velocities however, fans can likely be shut off due to their negligible effect when compared to freestream air velocity. Theoretically, due to the nature of EVs only creating thermal energy under load, fans should not be required at all as idling is not possible. As a result of thermal masses in the

system and potential low-speed driving not providing enough radiator airflow, they remain an option for an additional FOS.

The mass flow rate of air to the radiator is modeled by simply multiplying the car's velocity with the ambient air density at competition conditions, and dividing by 2 such that the air velocity is half of the vehicle's velocity. The airflow calculation operation is done through use of a Simulink subsystem, as is depicted in Figure 9.

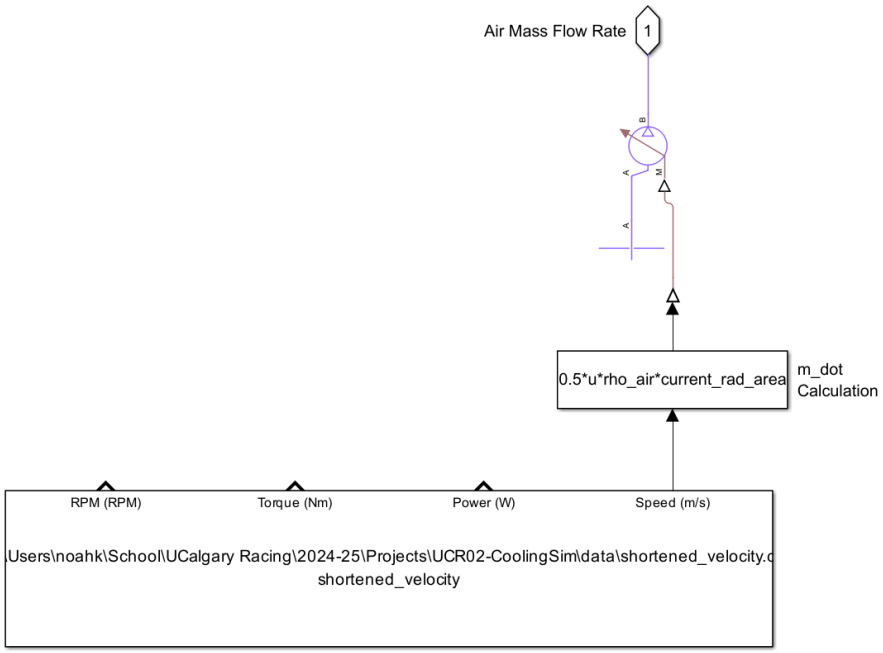

Figure 9: Radiator Airflow Calculation Subsystem

4.4 MATLAB Model Results

4.4.1 Final Model

With construction of individual component thermal models complete, a full TCS model is assembled. Different layouts, radiators, water flow rates, and air flow rates are evaluated and an optimal configuration is selected. A noteworthy challenge is encountered in importing the laptime simulation data to the *From Spreadsheet* Simulink block, as the maximum length of any dataset is the same as the maximum length in Microsoft Excel, slightly more than 1 million rows [21]. As such, a Python script is used to create lower-fidelity, longer time span datasets. An example of a configuration tested is seen in Figure 10.

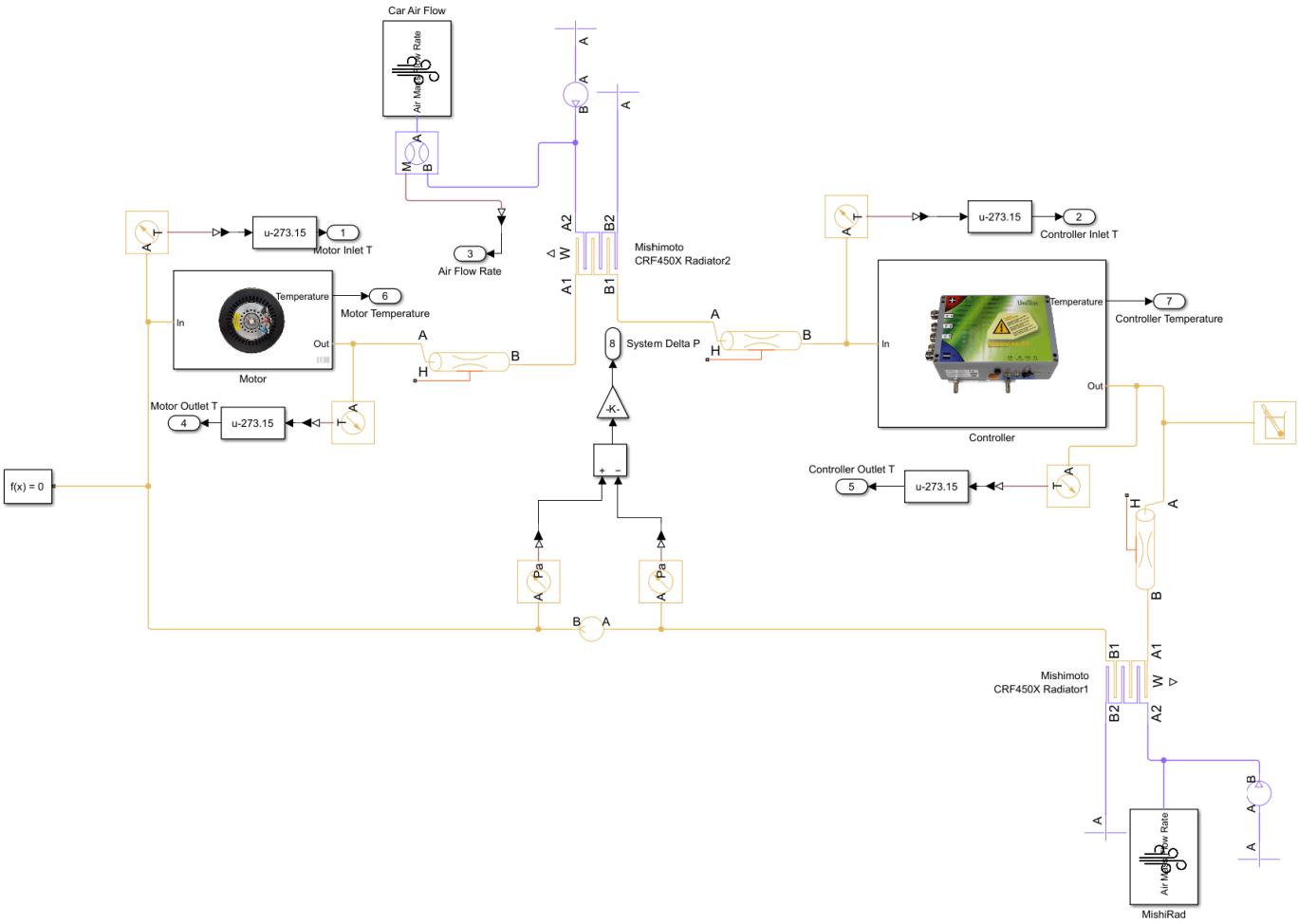

Figure 10: A Complete Configuration of the UCR-02 TCS Thermal Model

4.4.2 Layout Determination

An initial consideration when developing a TCS is the layout of the system. Some potential loop configurations are shown in Figure 11. Each configuration has different fluid flow, thermal, and physical characteristics. Due to the difficulty associated with bleeding a two-loop layout and its lack of distinct pressure drop or thermal advantages, it is impractical for implementation on the UCR-02. Furthermore, use of a single, large radiator is difficult due to packaging restrictions. As such, dual-radiator parallel and series layouts are thus evaluated from both performance and practicality perspectives.

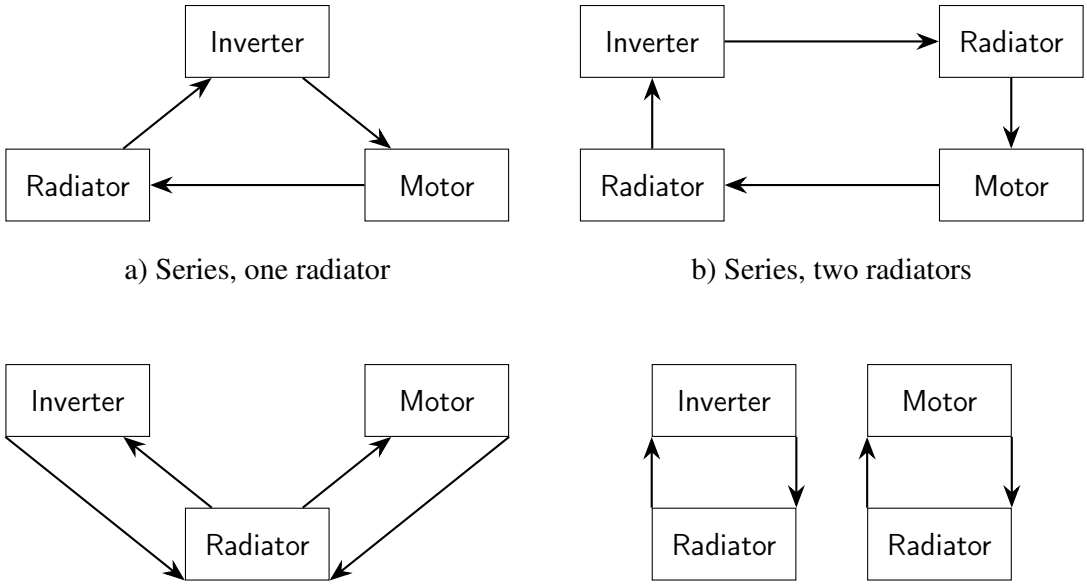

a) Series, one radiator

b) Series, two radiators

c) Parallel, one radiator

d) Two separate loops

Figure 11: Different configurations of cooling systems for inverters and motors.

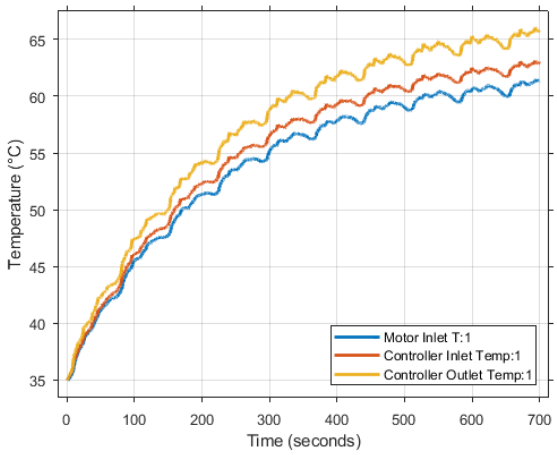

Figure 12: Series TCS Simulation Results

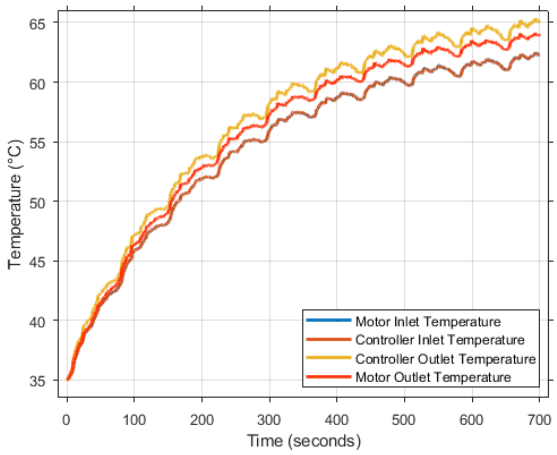

Figure 13: Parallel TCS Simulation Results

Simulation results for both parallel and series configurations can be seen in Figures 12 and 13. It is important to note that the temperatures achieved are merely for relative comparison, and have no intrinsic value. The parallel configuration offers consistent fluid temperatures to component inlets, however physical impracticalities such as the increased pressure drop due to splitting, cumbersome bleeding process, and inability to efficiently utilize multiple radiators make implementation of the

orientation difficult. Furthermore, the inverter has a maximum inlet temperature 15°C higher than that of the motor, and as such equal coolant delivery temperatures are unnecessary. A dual-radiator series configuration is therefore selected for use in the UCR-02 TCS.

4.4.3 Radiator Evaluation

With multiple radiator models created, evaluation of their heat dissipation begins. As the system uses a two-radiator series configuration, only relatively small radiators are evaluated. The radiators are attached to an air flow rate source, as well as the thermal components at the inlet with a constant flow rate. Temperature differences are then compared between the radiators as to compare their heat rejection capacity relative to each other, and radiators are then iterated through when determining the final configuration. Figures 14 and 15 show the temperature difference created by the generic computer radiator[15] and dirtbike radiator[19], respectively.

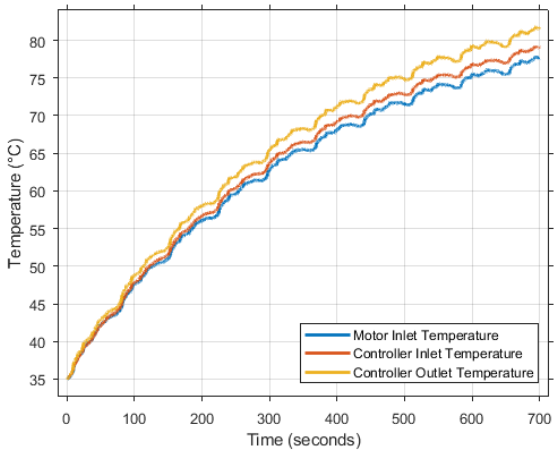

Figure 14: Generic Radiator Temperatures

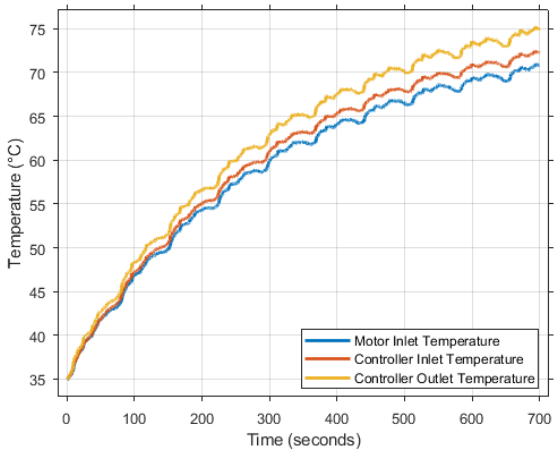

Figure 15: 450cc Dirtbike Radiator Temperatures

4.4.4 Final System Layout & Parameters

Iteration of different flow rates and radiators yields a final system design using two 450cc Mishimoto radiators [19], 6 lpm coolant flow rate, and minimum air mass flow rate of 0.1 kg/s. The results generated by the model can be seen in Figure 16. With air and coolant flow rates constrained, and radiators selected, appropriate fans and pumps can be selected through evaluating system pressure loss.

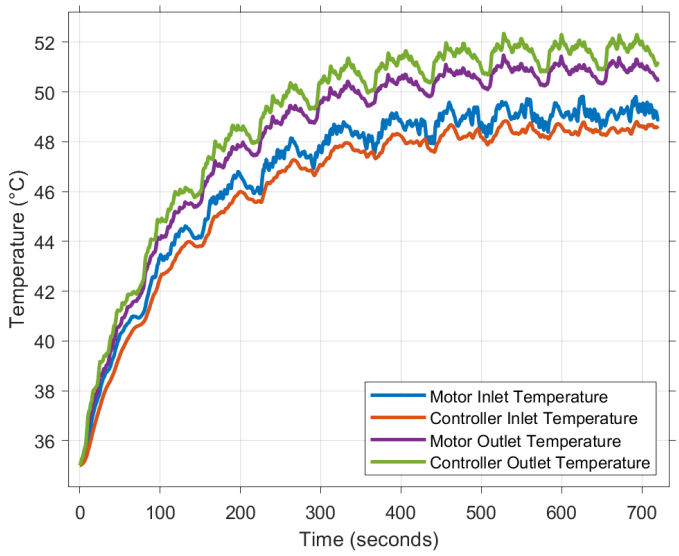

Figure 16: Final System Thermal Results

All final models, datasets, and scripts can be found in the project's GitHub repository[22] for future review.

4.5 Coolant-Side Pressure Drop Design

Although MATLAB Simulink has the Simscape fluids toolbox which supports liquid pressure drop design, the simplicity and flexibility of manual pressure drop calculations using Microsoft Excel makes it the preferred option. The motor and inverter are the two primary sources of pressure drop in the TCS loop, and their respective nominal pressure drops are provided by their manufacturers. Pressure drops at various flow rates were also empirically verified when developing the UCR-01, and can thus be used in the development of the UCR-02 TCS. The major and minor sources of pressure loss are combined to calculate total system pressure loss, and pumps are selected accordingly.

4.5.1 Component Testing

When developing the UCR-01 TCS, empirical verification of component coolant pressure drops was conducted by connecting each major component individually to a simple loop with a pump, a flow rate sensor, and pressure sensors to capture pressure drop at various flow rates. With raw pressure-flow rate data for both the motor and inverter collected as shown in Tables 2 and 3, the data is processed to provide pressure drops at various integer flow rates. The post-processed data yields pressure drops at potential UCR-02 TCS loop flow rates, which can be seen in Table 4.

Pressure Drop [bar]	Flow Rate [lpm]
0.0625	3.46
0.1188	4.82
0.1875	6.06
0.2563	7.32
0.3563	8.64
0.45	9.90
0.5813	11.20
0.5938	11.50

Table 2: Inverter Pressure-Flow Rate Data

Pressure Drop [bar]	Flow Rate [lpm]
0.0940	2.0027
0.1533	3.0055
0.2233	4.0000
0.3133	5.0027
0.4613	6.2011
0.6453	7.3994
0.7893	8.1983
1.0120	9.3966

Table 3: Motor Pressure-Flow Rate Data

Flow Rate [lpm]	Inverter Pressure Drop [bar]	Motor Pressure Drop [bar]
6	0.1800	0.4464
7	0.2387	0.5894
8	0.3056	0.7520

Table 4: Processed Pressure Drop vs. Flow Rate for the Motor and Inverter at 6–8 lpm.

A similar process as outlined above was followed for the custom UCR-01 radiators and a Mishimoto radiator of a comparable size to the aforementioned 450cc dirtbike radiator [19], which can be used to approximate other similar radiators when calculating overall system pressure drop.

4.5.2 System Pressure Drop Calculations

With component pressure drop values determined, basic pressure drop calculations for flow in a pipe are applied using a spreadsheet. The methodology employed uses loss coefficients to find pressure drop as a function of geometry and liquid flow rate. Fluid mechanics theory is beyond the scope of this report, however Dr. Paul Ziadé's fluid mechanics lectures cover the methodology used in great detail.[23] Combining a 3 metre estimate of the total tubing length used in the TCS with the number of contractions, expansions, elbows, and other fittings allows for an estimate of pressure drop due to tubing, whilst the empirical radiator, inverter, and motor pressure drops are imposed on the calculation. This yields a final estimate of TCS coolant pressure drop as shown in Table 5.

Pressure Drop [bar]	Flow Rate [lpm]
0.674	6
0.890	7
1.136	8

Table 5: System Pressure Drop Estimates at Various Flow Rates

Minor Losses										
Component	Type	D1 [mm]	D2 [mm]	Ratio	Relevant Velocity [m/s]	K_L	Head loss [m]	Quantity	Total Head Loss [m]	ΔP [bar]
Pump Outlet	Contraction	19.05	12.7	0.444444444	0.789411675	0.277261253	0.008806377	1	0.008806377	0.000863377
Pump Inlet	Expansion	12.7	19.05	0.444444444	0.789411675	0.394619761	0.01253392	1	0.01253392	0.001228826
Controller Fittings	90 Degree Elbow	12.7	12.7	1	0.789411675	0.4	0.012704807	2	0.025409614	0.002491159
Motor Inlet	Contraction	12.7	9.525	0.5625	1.403398534	0.20618826	0.020697933	1	0.020697933	0.002029225
Motor Outlet	Expansion	9.525	12.7	0.5625	1.403398534	0.283339411	0.028442648	1	0.028442648	0.002788517
Major Losses										
Component	Type	D [mm]	Velocity [m/s]	Re	ε [mm]	ε/D	f	length [m]	ΔP [Pa]	ΔP [bar]
Tubing Length	Smooth	12.7	0.789411675	9995.541652	0.002	0.00015748	0.032	3	235.5291187	0.002355291
Component Losses (Empirical)										
Component								Component ΔP [bar]	Quantity	Total ΔP [bar]
Bamocar D3								0.18	1	0.18
Emrax 228								0.4464	1	0.4464
Radiator								0.018	2	0.036
									Total ΔP [bar]:	0.674156395

Figure 17: Pressure Drop Spreadsheet

4.5.3 Pump Selection

With system pressure drop at various flow rates determined, pumps are selected. The pump selection process is multifactorial, as price, weight, and performance requirements must be met. The UCR-01 used two BLDC Pump Co. DC55B [24] pumps, however their power draw of 4.5A each meant that their use while the vehicle was driving was not possible. According to the pump performance curves provided by the manufacturer, one pump should be able to meet the minium 6 lpm requirement of the UCR-02's TCS.

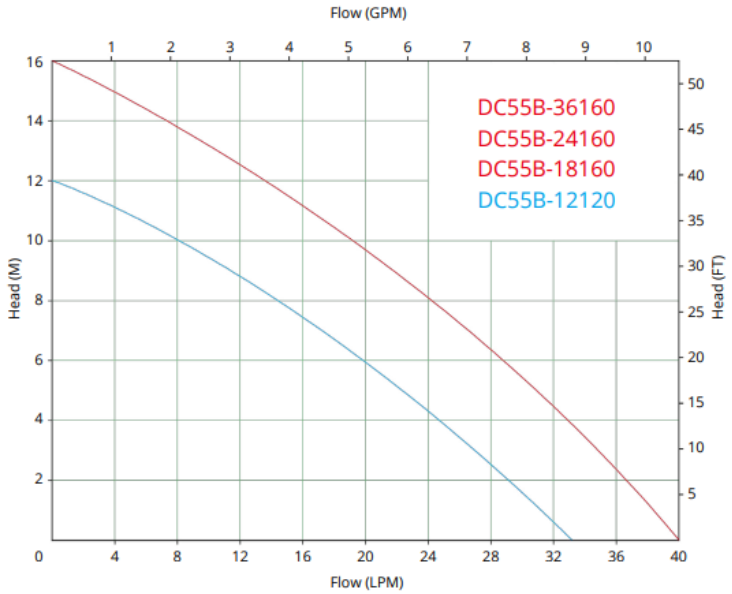

Figure 18: BLDC Pump Co. DC55B [24] Curves

As the team already had 3 DC55B pumps, empirical validation of their performance was conducted using a loop containing a flow rate sensor and the major components in series. One pump was unable to maintain flow through both components, suggesting either pump damage or manufacturer

error. The manufacturer specifies that a floating PWM signal should result in the pumps running at maximum power, and thus it can be concluded that PWM controlling is not the issue as the signal was left floating. Further, multiple DC55Bs were tested confirming that damage to a single pump is also not the issue.

By measuring flow rates through individual components, and then correlating to the pump performance curves and empirically verified pressure drops, it is determined that the pumps are capable of providing under 50% of the theoretical flow rate whilst still consuming up to 4.5A. To ensure the issue lies in the pumps and not the components having higher than previously determined pressure drops, Davies Craig EBP23s are used to flow water through each component, and their flow rates confirm the empirical data when correlated using the performance curves. Due to the insufficient performance of the DC55B pumps, alternative pumps are identified.

After researching and considering numerous pumps, the Davies Craig EBP40 [4] pump was selected for use on the UCR-02, potentially alongside a Davies Craig EBP23 [12] pump. From previous internal combustion cars, the team already possesses 3 EBP23 pumps which, although insufficient to flow the UCR-02 TCS coolant alone, can be used to boost system pressure alongside the larger EBP40 whilst minimally impacting low voltage power draw. Pump performance is determined using a performance curve as can be seen in Figure 19.

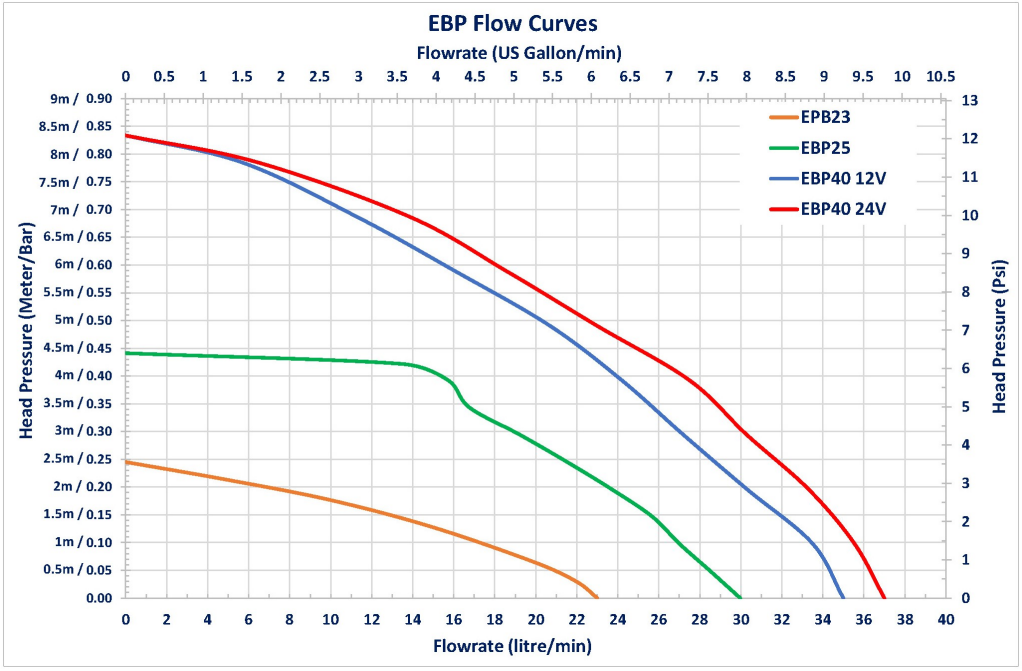

Figure 19: Davies Craig EBP Performance Curves [4]

The performance of the pump is determined by selecting flow rate (X axis) and finding the maximum head pressure the pump is capable of at the selected flow rate (Y axis). From Table 5, it can

be seen that the 12V EBP40 is theoretically capable of flowing the UCR-02 TCS alone. For an added layer of safety, a Davies Craig EBP23 can be added to the loop to increase head pressure further due to the pressure-boosting nature of pumps in series. This adaptable design makes implementing changes when testing considerably simpler, and allows for TCS pump power draw to be minimized.

4.6 Air-Side Pressure Drop Design

4.6.1 Radiator Pressure Drop

Determination of exact radiator air-side pressure drops is difficult for a variety of reasons, including their small size (typically in the hundreds of Pascals [Pa]), the cost and difficulty of performing CFD, and the necessity of a wind tunnel or similar setup to accurately measure pressure drop at various air flow rates. Although the drivetrain subteam is currently developing a rigorous radiator testing procedure and test stand to address these radiator verification issues, it will not be completed during the 2025 season. Due to the time-restricted nature of the UCR-02's TCS development, valid approximations must be used with a sufficient FOS to select appropriate fans.

The team already possesses SPAL VA39 [25] fans which can be used to roughly estimate the pressure drop of radiators. The SPAL fans were used in the UCR-01's TCS, however their current draw of up to 5 Amps is too high for use whilst the vehicle is driving. Further, their 140mm diameter is too large for the smaller UCR-02 radiators. A fan is attached directly to a radiator, without a shroud, and the velocity of air through the radiator is measured using an anemometer. This speed is used with the fan's performance curve to determine the pressure drop of the radiator core at that air velocity. The radiator has core geometry similar to most other radiators, with tubes 1.6mm wide, a depth of 40mm, and fins measuring 3.5mm peak to peak. The area of the fan is then calculated to find the pressure drop per unit core area, which is then used to find approximations of pressure drop in other radiators.

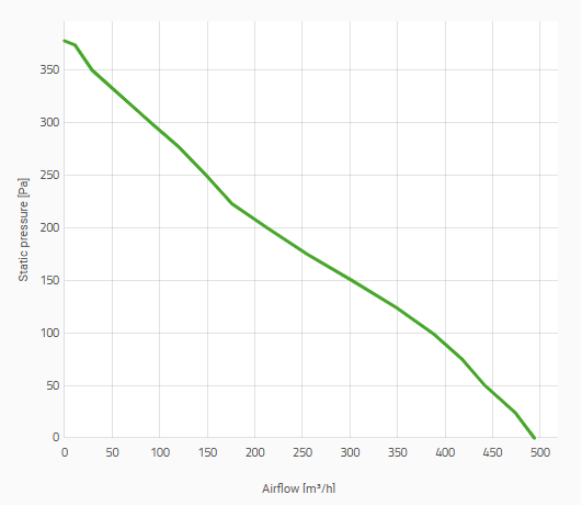

Figure 20: SPAL VA39 [25] Fan Performance Curve

It must be noted the described method of approximating air-side pressure drop is highly inaccurate as limitations such as the imperfect sealing of fan flow, anemometer inaccuracy, and differences in core geometry between radiators all add error to the obtained radiator pressure drop values. As such, a generous FOS of 1.75 is applied to the value. In future seasons, the improved radiator testing methodology being developed will address the inaccuracy of this method and improve TCS development.

At lower vehicle velocities, the fan's pressure rise is the dominant force causing air flow through the radiator. As vehicle velocity increases, dynamic pressure increases eventually making the fan redundant at high speeds. According to the Simulink model, and as confirmed by the nature of EV heat generation, fans on the UCR-02 may be unnecessary. The UCR-02's TCS, however, being the first optimized and functioning EV cooling system UCalgary Racing has developed, is designed to be more conservative and thus fans are included to add an additional FOS.

4.6.2 Fan Selection

Using the methodology previously outlined, a pressure drop estimate of roughly 140 Pa is obtained for the selected radiators at a flow rate of 5 m^3/min. Appropriate fans are thus selected based on these figures using fan performance curves, which function similarly to pump performance curves. The NMB Technologies 12038VE [26] is identified as an appropriate fan for the radiators due to its compact 120 mm square chassis, maximum current draw of 3.2 A, IP68 waterproof rating, and competitive price.

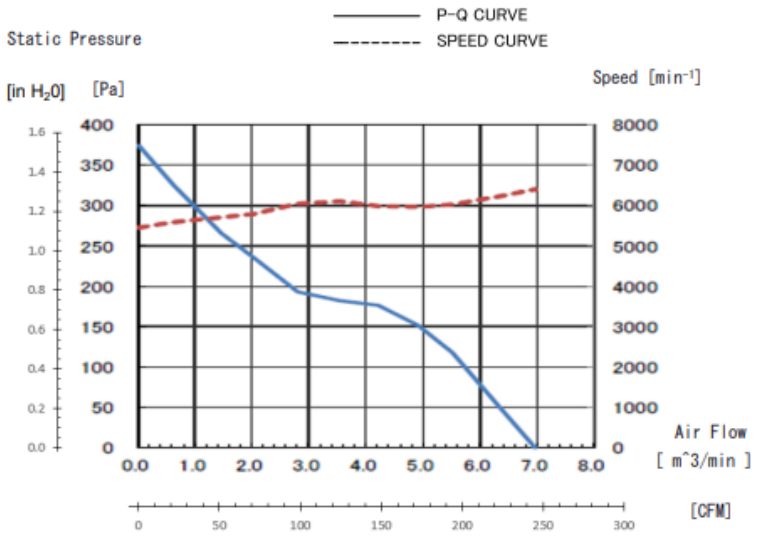

Figure 21: NMB 12038VE [26] Fan Performance Curve

As can be seen from Figure 21, the NMB 12038VE fans meet the flow rate and pressure requirements for fans to be effective. As such, they are selected for use in the UCR-02's TCS.

4.6.3 Fan Shroud Design

To maximize heat transfer, it must be ensured that the fans pull air through the entire radiator core area. A fan shroud is a simple and effective way of achieving this, and thus a fan shroud design is created. Creating the geometry is simple, as the square nature of the fan means the shroud is merely a loft between the radiator shape and fan shape, with fillets to round sharp edges.

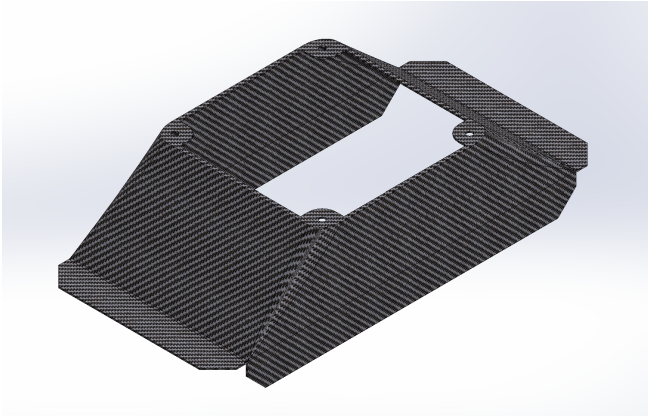

Figure 22: CAD Model of the Fan Shroud

This basic shape is then optimized to be manufactured in carbon fiber by creating a mold model which is 3D printed. A simple aluminum bracket is also designed to ensure safe bolting of the fans onto the shroud.

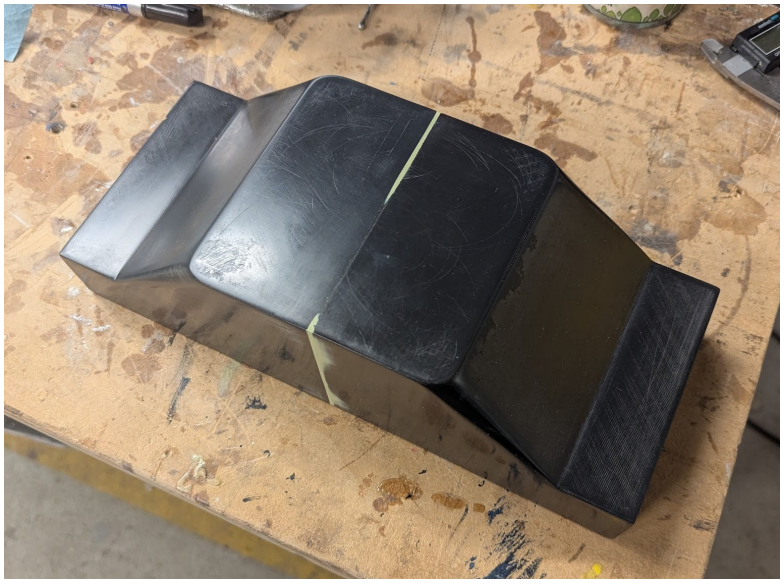

Figure 23: Fan Shroud Mold, 3D Printed, Sanded, and Waxed

The carbon fiber shroud can now be manufactured and used on the UCR-02.

4.7 Sensors & Data Collection

To inform future TCS design processes, the system is designed with integrated data collection devices. Coolant flow rate and pressure should be constant, predictable variables and thus do not need to be gathered while competing. Coolant temperature is left as being a variable of great importance, with the 4 major points of concern being the radiator inlets and outlets. Appropriate sensors are thus identified, with the final TCS using Amphenol GE-2102 [27] sensors due to their price, weight, and 1/2 inch fitting size.

5 System Construction and Assembly

5.1 Radiator Modifications

In order to use the Mishimoto [19] radiators selected in Section 4.4.4, some basic modifications must be made. The radiators' integrated mounting tabs are removed as they are not used for mounting on the UCR-02 and interfere with fan shroud fitment. Holes are then drilled in the top of the radiators, and aluminum bungs are welded in. The bungs are threaded aluminum adapters that allow for a removable plug to be screwed into to the radiator. The bungs are opened when bleeding the TCS, as they allow air to escape from the radiators. Further, the bungs can also be used to add additional sensors directly to the radiators when testing, such as pressure and temperature.

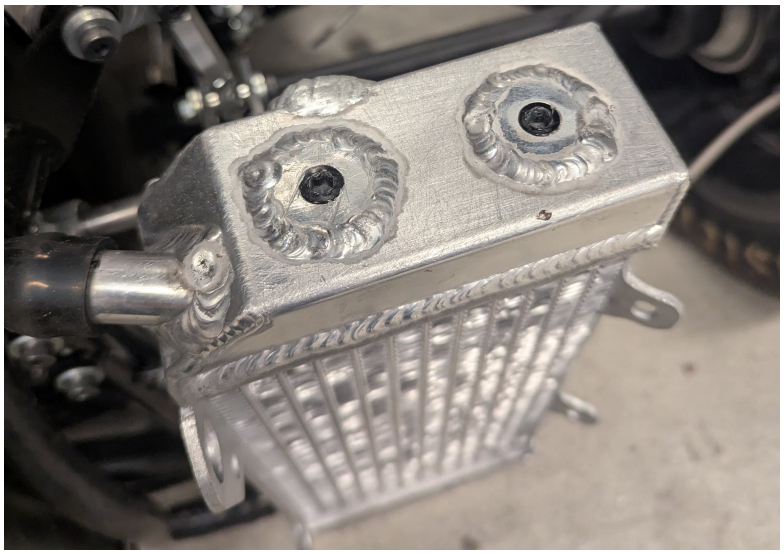

Figure 24: UCR-02 Radiator Bungs, Welded in and Plugged

5.2 Component Placement

Although placement of TCS components are restricted by the thermal design of the loop, their physical positions are optimized for bleeding and integrated with non-TCS components.

5.2.1 Radiators

Radiator placement is predetermined by CFD as discussed in Section 4.3.5, and thus they are placed on the rear plane of the vehicle. Tabs are welded on the frame and radiators accordingly, and the radiators are bolted on in their final locations.

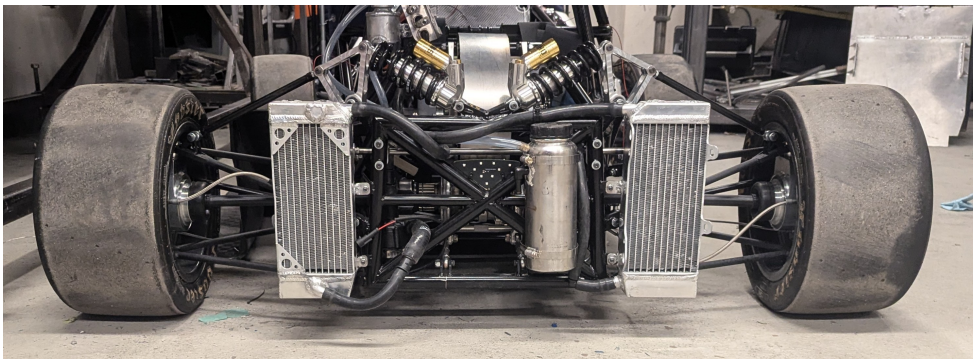

Figure 25: The Radiators in their Final Locations on the UCR-02

5.2.2 Pump

To aid the bleeding process and prevent the pump from stalling, the pump should be the lowest point in the TCS. As such, the pump is placed inboard at a rear corner of the frame such that its inlet is always saturated with water as air will rise to the highest point in the loop. A simple bracket is designed and welded on to the frame to help secure the pump, hose clamps are used to fix the pump in place.

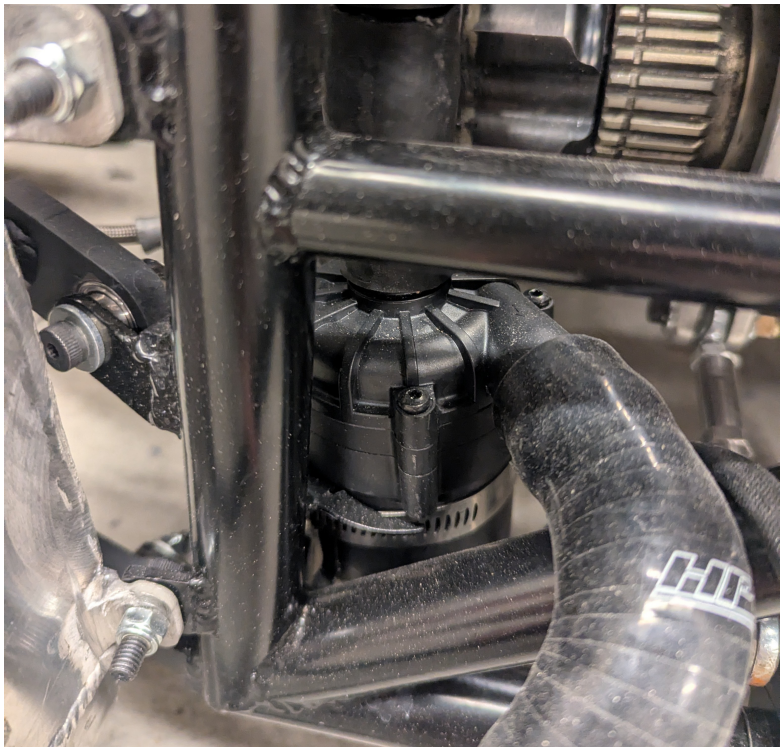

Figure 26: The Davies Craig EBP40 Fixed on the UCR-02 Frame

5.2.3 Filler Pot

To fill the closed loop with coolant, a filler pot is plumbed in to the pump inlet line. The filler pot is mounted such that it is the highest point in the TCS loop allowing air to escape and water to enter the loop at the pump inlet.

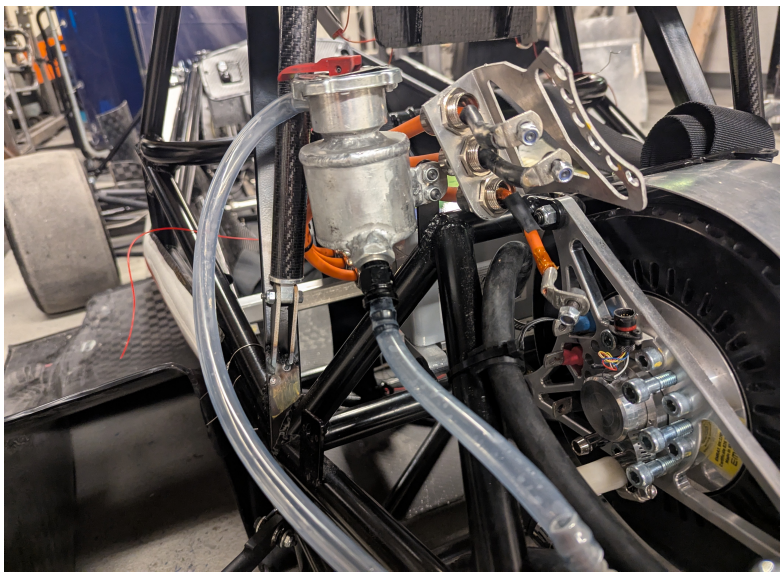

Figure 27: The Filler Pot Plumbed in to the UCR-02 TCS

The filler neck is sealed by a radiator cap with an integrated pressure release valve, which allows steam to escape the system in the event of overpressurization. The escaped steam vents into the catch can, which is mounted to the rear of the vehicle.

5.3 Tubing and Routing

5.3.1 Tube Selection

The UCR-01 TCS used stiff, 3/4 inch rubber tubing which was difficult to route due to its tendency to kink when bent. As a result of the adaptability of softer tubing, it is preferred for use on the UCR-02's TCS. The use of softer tubing is enabled by the low pressure of the system, and the main line diameter is selected to be 1/2 inch. Some TCS components such as the pump and motor use different tubing sizes, however these components are adapted to the 1/2 inch main line diameter as soon as possible. The tubing selected was soft latex tubing [28], rated for a maximum pressure of 1.73 Bar whilst still being flexible.

5.3.2 Routing of Tubing

With components placed, the final physical loop configuration is determined to minimize tubing length.

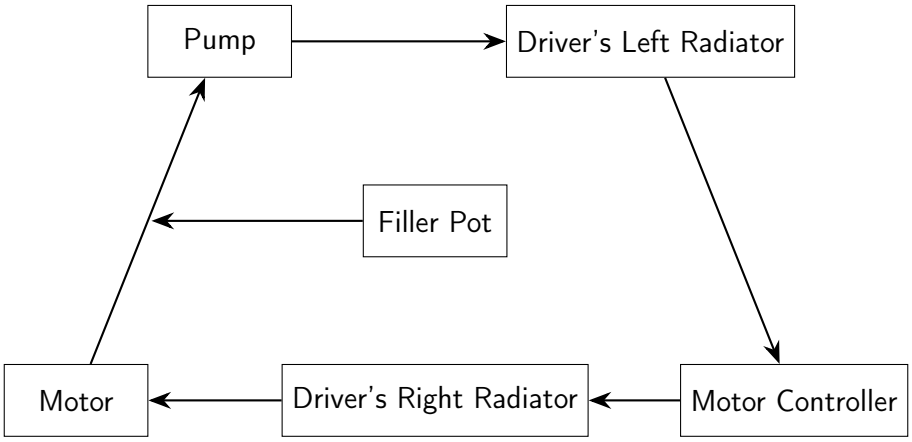

Figure 28: Final Physical TCS Loop Orientation

A challenge encountered is that the 1/2 inch main line tubing used in the UCR-02's TCS is too soft for routing, so 90°elbows are used at any sharp corners to prevent kinking. Further, the tubing must be firmly secured and fixed to the frame to ensure there is no motion and potential kinking under dynamic conditions. Tube organizers are thus 3D printed, and the tubes are all attached with hose clamps to ensure complete system isolation.

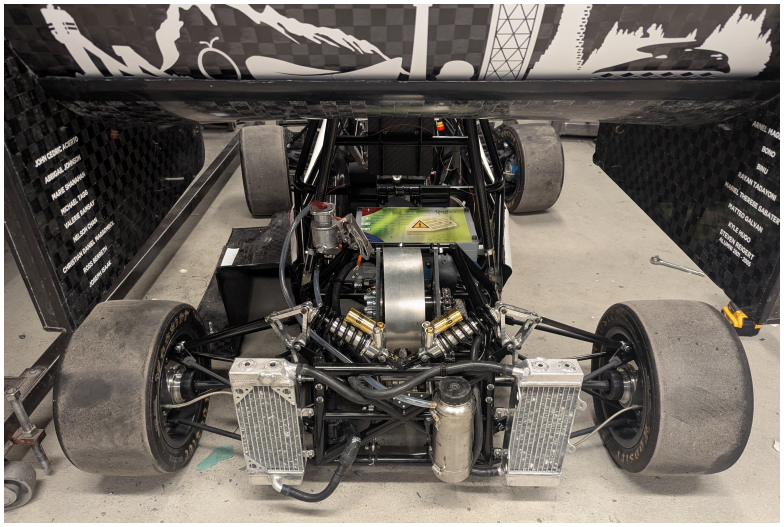

Figure 29: The UCR-02 TCS In-Frame

6 Testing & Validation

6.1 Off-Vehicle Testing

Before assembling the loop on the car, the loop is preliminarily assembled to conduct basic flow rate and heat transfer testing.

6.1.1 Flow Rate Testing

5 Off-car coolant flow rate testing is a straightforward process, as all TCS components are connected in series with a Davies Craig EBP40, and flow rate is measured by collecting and weighing fluid throughput during a measured time interval.

Figure 30: The Liquid Flow Rate Test Setup

The results of this process reveal a flow rate of around 6 lpm, verifying the pressure drop calculations discussed in Section 4.5.2.

6.1.2 Heat Transfer Testing

Evaluating heat transfer of a radiator accurately and in a manner which produces generalizable data requires a high-precision laboratory environment, however basic heat transfer testing can be done relatively accurately with simple tools. A problematic method is outlined in Section 4.2.2, with the

main issues being poor temperature control and recirculation of radiator-cooled water back into the heated water supply. To accurately evaluate the heat transfer capacity of the radiators and fans selected, an isolated, isothermal hot water reservoir must be established. A sous vide machine is typically used to cook meat, however its ability to hold water at a constant temperature and circulate it makes it a suitable device for hot water reservoir heating. As such, a 10 liter volume of water is placed in a container and heated with the sous vide machine, and a temporary shroud is attached to seal the fan to the radiator. The radiator is then connected to a pump and tubing, and upon the machine heating the water to the desired temperature the pump flows water through the radiator with an active fan and expels it to a second reservoir. An in-line temperature sensor is added to the radiator outlet tubing for data collection, and flow rate is manually measured by a timed mass test.

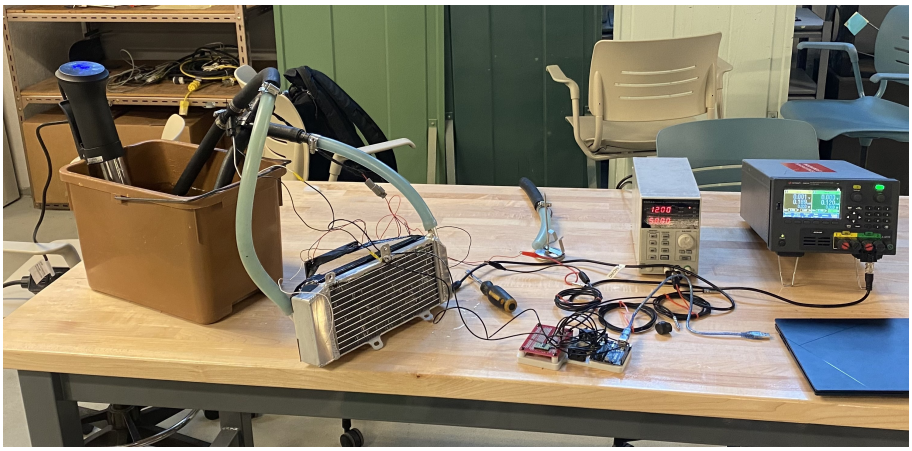

Figure 31: The Heat Transfer Evaluation Setup

The testing apparatus is run at various inlet temperatures, and the collected temperature and flow rate data is used to evaluate heat transfer capacity of the specific radiator and fan setup.

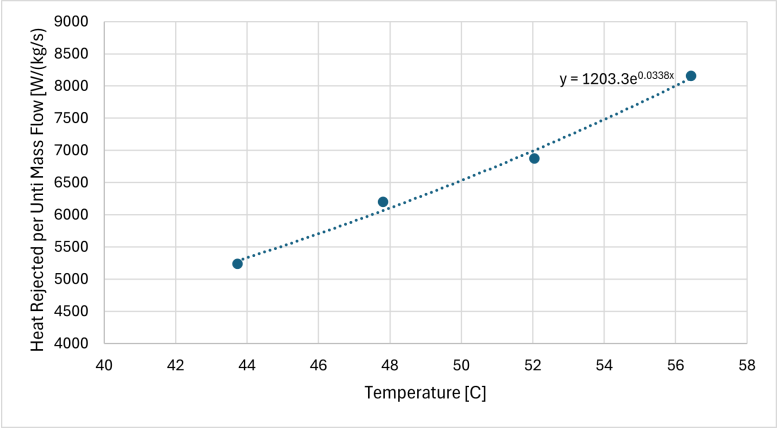

Figure 32: Radiator and Fan Combined Heat Transfer Plot

The results obtained from this process reveal a static vehicle heat transfer capacity of 1000W at 6 lpm and 50°C inlet temperature, and are used to generate the plot seen in Figure 32.

6.2 On-Vehicle Static Testing

6.2.1 Flow Rate and Bleeding Testing

With TCS component placement and off-vehicle testing complete, the TCS is assembled in the car's chassis. A test to determine bleedability and flow rate is then conducted, with the system proving exceptionally difficult to bleed. The pump was audibly encountering air bubbles, and running in such a state compromises heat transfer, coolant flow rate, and pump longevity through cavitation. Further, as a result of the extra fittings and air trapped in the system, the flow rate is compromised to approximately 4.5 lpm as measured by an in-line flow sensor. The flow rate sensor is calibrated by running a single pump through the device and manually conducting a timed mass flow test. Upon performing a manual mass flow test, a flow rate of 5.5 lpm is revealed which, although not ideal, is acceptable and calls the accuracy of the sensor into question. As a result of the challenges encountered upon in-chassis TCS assembly, minor TCS loop changes must be made. Fortunately, the built-in modularity of the TCS makes implementing the necessary changes simple.

6.2.2 Modifications

To address the issues discovered in Section 6.2.1, a swirl pot is added to the system to expel air effectively. A prototype swirl pot is 3D printed to ensure it addresses the issue of trapped air, and replaces the filler pot. The swirl pot receives coolant at the highest point in the system, creates a vortex, and drains into the pump inlet. The vortex created and positions of the swirl pot ports allow expulsion of air when bleeding.

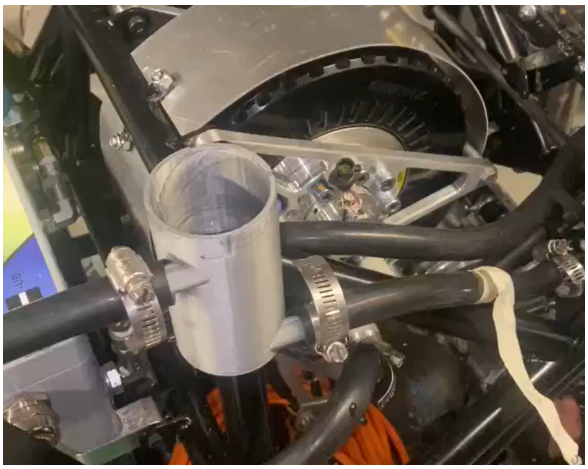

Figure 33: Prototype Swirl Pot in Frame

The 3D printed swirl pot yields exceptional results, allowing the system to be bled in a matter of minutes. As such, an aluminum swirl pot is designed and manufactured to be used in the final UCR-02 TCS. The swirl pot is sized at 0.3 liters such that it does not starve the pump of coolant under acceleration, and a pressure-release radiator cap venting to the catch can ensures the system is not pressurized past the tubing's maximum rating.

<pic of final swirl pot>

The final system loop and component order can be found in Figure 34, and the final assembled TCS in frame can be found in Figure 35.

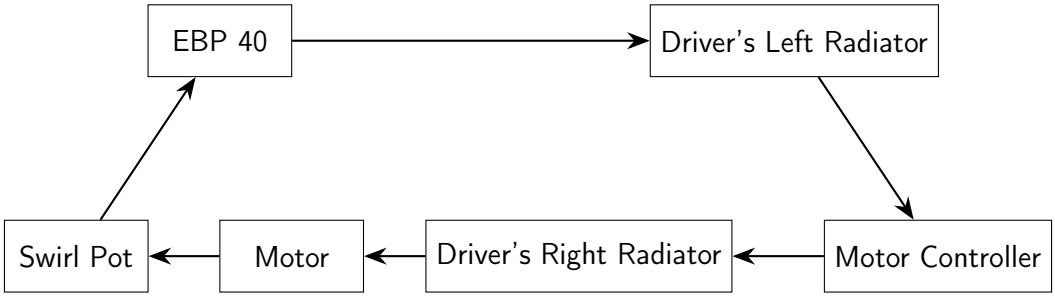

Figure 34: Final Physical TCS Loop Orientation

Figure 35: Final TCS In-frame

6.3 On-Vehicle Dynamic Testing

As of the writing of this report, high-quality on-vehicle dynamic testing has not been done on the UCR-02. The lack of testing is mainly due to delays in implementation of a functional low-voltage system, and as such I am currently working on a placeholder system to acquire useful data. Upon collection of the data, this and subsequent sections will be completed accordingly.

7 Conclusion

While the TCS outlined in this report has not been validated to the extent desired, it represents a significant step forward in terms of weight savings, power draw minimization, and benchtop validation. Upon collection of active vehicle testing data, the report will be expanded to present and analyze the results of the project and suggest future improvements. The systems bottlenecking evaluation of the TCS are beyond the scope of this report and project, however upon releif of the bottleneck useful data should be collected. While ideal future TCS developments would include the removal of fans, decreasing of radiator size, and placement of radiators in sidepods, such design decisions require in-depth data collection and analysis to validate them; as such they are merely speculative until proven.

Nomenclature

ϵ -NTU	Effectiveness - Number of Transfer Units
CFD	Computational Fluid Dynamics
EV	Electric Vehicle
FOS	Factor of Safety
FSAE	Formula SAE
ICE	Internal Combustion Engine
LMTD	Log-Mean Temperature Difference
lpm	Litres per Minute
Pa	Pascals
PDE	Partial Differential Equation
TCS	Tractive Cooling System

References

[1] F. SAE, "Formula sae 2025 rules." https://www.fsaeonline.com/cdsweb/gen/DownloadDocument.aspx?DocumentID=4bafd174-62da-48b6-b016-589385ca5ae6. Accessed: 2025-03-27.

[2] F. Jander, "Designing a Formula SAE Electric Cooling System." https://www.filipjander.com/2020/09/designing-formula-sae-cooling-system.html. Accessed: 2025-03-17.

[3] Mishimoto, "Kawasaki kx450f aluminum dirt bike radiator (left braced)." https://www.mishimoto.com/kawasaki-kx450f-aluminum-dirt-bike-radiator-10-left-braced.html. Accessed: 2025-03-17.

[4] Davies-Craig, "Ebp-40 electric booster pump (12v)." https://daviescraig.com.au/product/ebp40-electric-booster-pump-12v-9040. Accessed: 2025-03-17.

[5] Sanyo-Denki, "San ace 120wv38 cooling fan datasheet." https://www.mouser.com/datasheet/2/471/San_Ace_120WV38_E-1282467.pdf. Accessed: 2025-03-17.

[6] J. LaMarre, "FSAE Electric Vehicle Cooling System Design." https://ideaexchange.uakron.edu/cgi/viewcontent.cgi?article=1143&context=honors_research_projects. Accessed: 2025-03-17.

[7] GRI-Pumps, "INTG7 Series Technical Specifications." https://www.gripumps.com/media/1156/gri-intg7-series-0519.pdf. Accessed: 2025-03-17.

[8] Shubhankar Jamdar, Ruturaj Yawale, Manas Kolhe, Atharva Hood, Nilesh Gaikwad, "Design and manufacturing of cooling system for FSAE car." https://doi.org/10.1016/j.matpr.2022.12.058. Accessed: 2025-03-17.

[9] Harriet Alicia Chiu, "Design of a FSAE Cooling System." https://dspace.mit.edu/handle/1721.1/123258. Accessed: 2025-03-17.

[10] Mishimoto, "Aluminum Radiator, fits Yamaha YFM700R Raptor 2006-2012." https://www.mishimoto.com/yamaha-yfm700r-raptor-aluminum-radiator-06-11.html. Accessed: 2025-03-17.

[11] Everflo, "EF7000 7.0GPM Diaphragm Pump." https://everflopump.com/product/ef7000-7-0-gpm-diaphragm-pump/. Accessed: 2025-03-17.

[12] Davies-Craig, "Ebp-23 electric booster pump kit (12v)." https://daviescraig.com.au/product/ebp23-electric-booster-pump-kit-12v-9050. Accessed: 2025-03-27.

[13] Unitek, "Bamocar d3 motor controller." https://www.unitek-industrie-elektronik.de/produkte/bamocar-d3/. Accessed: 2025-03-27.

[14] EMRAX, "Emrax 228 electric motor." https://emrax.com/e-motors/emrax-228/. Accessed: 2025-03-27.

[15] AliExpress, "Pc water cooling radiator." https://www.aliexpress.com/item/1005005795094995.html?spm=a2g0o.productlist.main.1.1a6857ddOyT73i&algo_pvid=64c6059d-c587-4c86-bf2a-c8be9d709fb1&pdp_ext_f=%7B%22order%22%3A%22833%22%2C%22eval%22%3A%221%22%7D&utparam-url=scene%3Asearch%7Cquery_from%3A. Accessed: 2025-03-27.

[16] MathWorks, "Matlab product page." https://www.mathworks.com/products/matlab.html. Accessed: 2025-03-27.

[17] MathWorks, "Formula student michigan." https://www.mathworks.com/academia/student-competitions/formula-student-michigan.html. Accessed: 2025-03-27.

[18] MathWorks, "Modeling heat exchangers." https://www.mathworks.com/help/hydro/ug/modeling-heat-exchangers.html. Accessed: 2025-03-27.

[19] Mishimoto, "Honda crf450x left braced aluminum dirt bike radiator (2005-2013)." https://www.mishimoto.com/honda-crf450x-left-braced-aluminum-dirt-bike-radiator-2005-2013.html. Accessed: 2025-03-27.

[20] Mishimoto, "Yamaha yxr700 rhino aluminum radiator (2008-2011)." https://www.mishimoto.com/yamaha-yxr700-rhino-aluminum-radiator-08-11.html. Accessed: 2025-03-27.

[21] Microsoft, "Excel specifications and limits." https://support.microsoft.com/en-us/office/excel-specifications-and-limits-1672b34d-7043-467e-8e27-269d656771c3. Accessed: 2025-03-27.

[22] N. Elsayed, "Ucr02 cooling simulation." https://github.com/noahkae/UCR02-CoolingSim. Accessed: 2025-03-27.

[23] P. Ziadé, "Fundamentals of fluid mechanics." https://youtube.com/playlist?list=PLFc_srpNhmDxSYf2PffUPCwnYzV_otMU7&feature=shared. Accessed: 2025-04-17.

[24] B. P. Co., "Dc55b brushless dc pump datasheet." http://bldcpump.com/downloads/BLDC%20PUMP%20DC55B.pdf. Accessed: 2025-05-01.

[25] S. Automotive, "Va39-a100-45a 12v axial fan." https://www.spalautomotive.com/en/axial-fans?productcode=va39-a100-45a&articleid=33469. Accessed: 2025-05-01.

[26] N. T. Corporation, "12038ve-12r-gue-4 dc axial fan datasheet." https://nmbtc.com/wp-content/uploads/parts/documents/12038VE-12R-GUE-4%20data%20sheet.pdf. Accessed: 2025-05-01.

[27] A. A. Sensors, "Thermometrics ctts flow-through temperature sensor datasheet." https://www.amphenol-sensors.com/hubfs/Documents/AAS-930-235A-Thermometrics-CTTS-041119-web.pdf. Accessed: 2025-05-01.

[28] McMaster-Carr, "5234k55 latex tubing." https://www.mcmaster.com/5234K55/. Accessed: 2025-06-08.